

Chapter 3

Experimental setup

This chapter introduces the reader to the setup used in the experiments. The important and unique aspects of the setup are described. The chapter on generation and characterization of light pulses is extended, since the NOPA and FROG setups used, were in part developed within the thesis work. For the theoretical background on nonlinear optics the reader is referred to the literature on the special subjects. Some footnotes are included to give helpful hints to those who work with this or similar systems in the future.

3.1 Ultrahigh vacuum (UHV) setup and cryostat

The set-up comprises a mixing chamber (I) and a sample chamber (II) made from stainless steel (see Fig. 3.1). The vacuum is established by turbo molecular pumps with rotary pumps for the pre-vacuum. The background pressures are 10^{-6} and 10^{-8} mbar, respectively. Pressure reduction valves connect the mixing chamber with the high-pressure bottles with high purity gases, *Ar* (200 bar, 99.9999%), *Kr* (200 bar, 99.998%), *ClF* (30 bar, 99% from ABCR) and *Cl₂* (30 bar, 99%). All gases are used without further purification although in the future it may be desirable to purify the *ClF*. This has not been tried yet, because the chemical equilibria mentioned in chapter 2.4.1 may again lead to *Cl₂* formation. A needle valve controls the gas flux from the mixing chamber to the sample chamber.

The sample chamber is equipped with two *CaF₂* substrates that are thermally contacted with two independent sample holders, made from copper. One is attached to a flow cryostat, the other to a closed-cycle cryostat. In most experiments the flow cryostat is employed, since it can cool the sample down to 4 K. The temperature is checked with a Si-diode from Cryophysics. The two samples are thermally insulated from each other. They can be moved with the x-y-z manipulator holding the flow cryostat. The cycle cryostat is connected to the sample holder with flexible copper wires from the side, which limits the temperature to 20K¹. This setup allows switching between the cycle cryostat for long term experiments and the He-flow cryostat without opening the vacuum chamber.

A similar setup with a closed cycle cryostat is used for the preparation of *I₂* in *Kr* matrices [32, 144] from the vapor pressure above a solid *I₂* crystal (99,999% from Sigma Aldrich) and *Kr* (99,998% from Linde). The background pressures were 10^{-6} mbar in the mixing chamber² and $5 \cdot 10^{-9}$ mbar in the sample chamber. This low background pressure allows the samples to be kept for several days without noticeable changes.

¹This can be improved with a refurbished cycle cryostat.

² 10^{-6} mbar can be achieved by applying the turbo molecular pump but usually the 10^{-2} mbar produced with the rotary pump are sufficient, since *I₂* fluorescence is much stronger than that from all impurities. It was tested that the results are not affected by the impurities. Most of the molecules expected to be present in the background gas are not resonant with the used laser pulses.

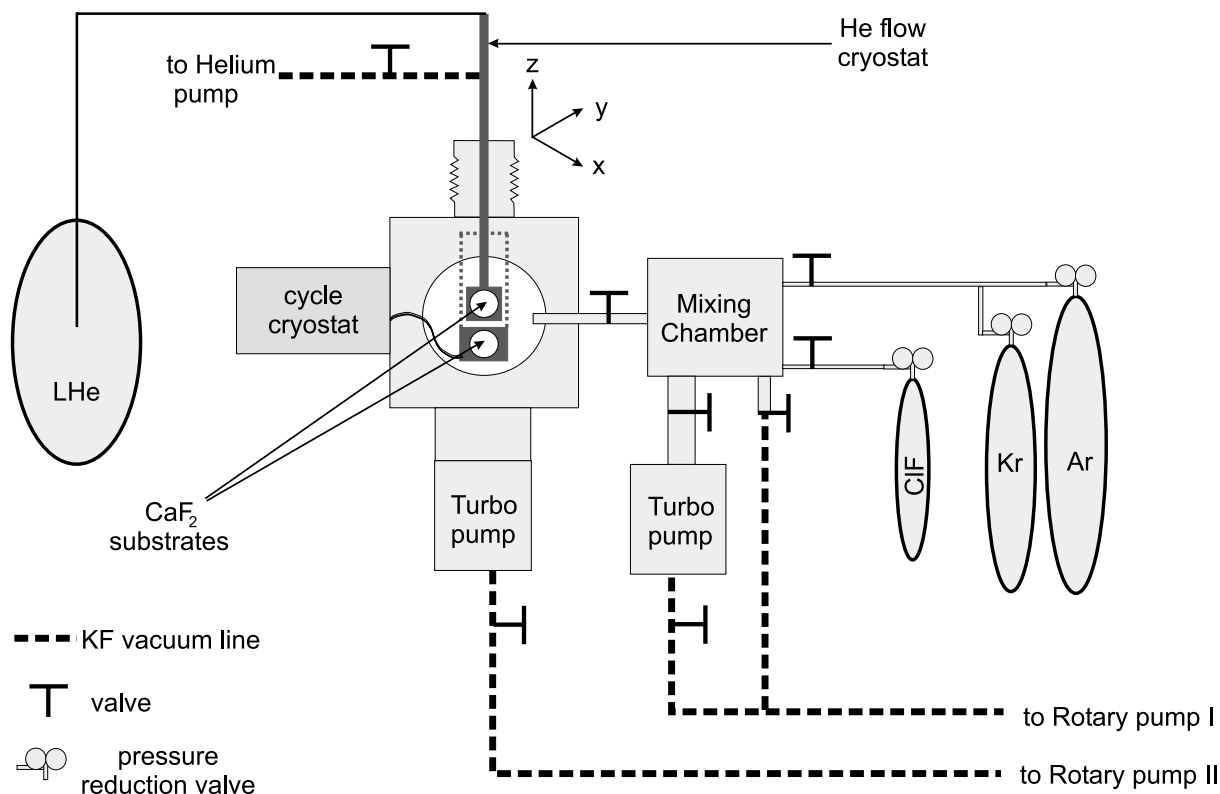


Figure 3.1: The sample chamber contains the two CaF_2 substrates, which can be moved with the x-y-z stage. The He-flow cryostat cools the upper substrate, while the lower substrate is connected to a cycle cryostat with flexible copper wires. The gas mixture (prepared in the mixing chamber) is sprayed onto the samples through the thin tube, which connects the two chambers. A top view of the geometry of the substrate, the thin tube and the laser beams is shown in Fig. 3.5. Besides the three connections to the ClF , Ar and Kr gas bottles, there are two more (not shown) to attach Xe and Cl_2 bottles.

3.2 Sample preparation

The mixing chamber is kept permanently passivated with ClF . Before diluting 1 mbar ClF with the rare gas at ratios ranging from 1:500 to 1:100,000 the mixing chamber is evacuated to a pressure of approx. 10^{-6} mbar. The mixture is introduced into the sample chamber (background pressure in the sample chamber is 10^{-8} mbar) through a stainless steel valve with a thin tube attached to it and sprayed onto a 1 mm thick CaF_2 substrate. The geometry for the crystal growth is depicted in Fig. 3.5. The tube is at the same height as the laser beams. Thus the sample does not have to be moved after preparation. Rare gas films of typically 100 μm thickness are grown in 30 min, which has been verified by counting interference fringes of a HeNe laser. The quality of the films is judged by eye and by the scattering of UV pulses. The deposition conditions (rate and temperature) have been optimized to generate transparent and only weakly scattering films. The rate is controlled with the needle valve and checked with the ionization manometer, which reads 10^{-5} mbar during deposition, reflecting the dynamical equilibrium with the cryostat and the turbo pump. The temperature is set to 15 K for Ar and 20 K for Kr matrices. The temperature of the samples must subsequently be changed quite slowly to avoid cracks in the film due to thermal expansion or contraction. If the samples are deposited more rapidly or at lower temperatures, this usually leads to scattering films with many cracks. Higher temperatures have the disadvantage of promoting the formation of molecular dimers and higher clusters.

Most of the experiments on Cl_2 were conducted in the ClF/Ar or ClF/Kr samples. The 1% content of Cl_2 in the ClF gas is sufficient, since the absorption cross section for Cl_2 is much larger (cf. Fig. 2.12). To check the assignment of the bands and dynamics to Cl_2 , pure Cl_2/Ar samples were grown at similarly low concentration from 1:10 000 to 1:100 000. For this purpose, gas from a high pressure bottle with 1:100 Cl_2/Ar was diluted with Ar .

The I_2/Kr samples consisting of 30 μm thick clear crack-free films of Kr doped with I_2 in a ratio of 1500 : 1 were prepared in the same way at 20 K as described in refs. [32, 144].

3.3 Laser system

A commercial regeneratively amplified Ti:Sa laser, (CPA 2001 from Clark-MXR) is the basis of all fs pulses used in this work. It delivers pulses at 775 nm with a pulse duration of 150 fs at 1 kHz repetition rate and with a typical pulse energy of 750 μJ . This laser is seeded with a frequency doubled Erbium fiber laser pumped with telecom diode arrays. It is a turn key system but has the disadvantage that the wavelength cannot be tuned. All tunable radiation is generated by subsequent nonlinear processes. Fig. 3.2 shows the setup in a block diagram.

At the moment four non-collinear optical parametric amplifiers (NOPAs) are pumped in parallel. The remaining fraction of fundamental laser light is used for second harmonic generation (SHG) and for white light generation in another experiment. This extremely flexible setup was made possible by a great increase of NOPA efficiency achieved in this thesis (chapter 3.4). The chirp of the fundamental at 775 nm is adjusted to produce a high conversion efficiency in all four NOPAs at the same time. The pulses are slightly negatively pre-chirped (blue components first) when leaving the CPA 2001, since there is some dispersive material before the NOPAs.

3.4 New NOPA design

The first NOPA [183] setup goes back to 1997 and since then many groups improved various parameters [34, 35, 184, 185]. The major advantage of the new design presented in this thesis is that the efficiency of the process is doubled while excellent pulse stability and temporal characteristics are maintained for the same output power. In this way the NOPAs are now pumped with pulse energies of only 0.11 mJ . The commercial regeneratively amplified Ti:Sa laser delivers approximately 0.7-0.8 mJ and up to six of these devices can be pumped in parallel, while retaining some excess of pump-power e.g. for SHG. In addition, the new NOPA is much more compact (300 x 600 mm instead of 600 x 1200).

The wavelengths of the NOPA are readily tuned, rendering this device a very versatile spectroscopic tool. It is tunable from 460 to 720 nm, and it delivers 10 μJ pulse energy around 550 nm, thus providing an excellent overall efficiency of about 10 %. The used pulse length was typically 30 fs and with an optimized alignment pulses shorter than 20 fs can be obtained [35]. If one aims at records concerning pulse duration < 20 fs, the spectral bandwidth of the NOPA becomes very broad. These pulses are less useful for the spectroscopic applications of this thesis.

3.4.1 NOPA setup

The non-collinearly pumped optical parametric amplifiers (NOPA) in Fig. 3.3 closely follows the original design developed in the group of Riedle [183]. The pump light (110 μJ of the CPA output) is mildly focused with a 2 m lens, approx. 1 m before the NOPA (not shown in Fig. 3.3)³. A fraction of 4% is reflected off the beamsplitter (BS), focused with a 30 mm lens (L1) into a 1mm thick sapphire plate and a second 3 mm quartz lens (L2) collects the divergent white light, generated in the sapphire (Saph), and mildly focuses it into the NOPA BBO. This beam is kept parallel to the

³Alternatively a telescope setup that produces the same convergence can be used.

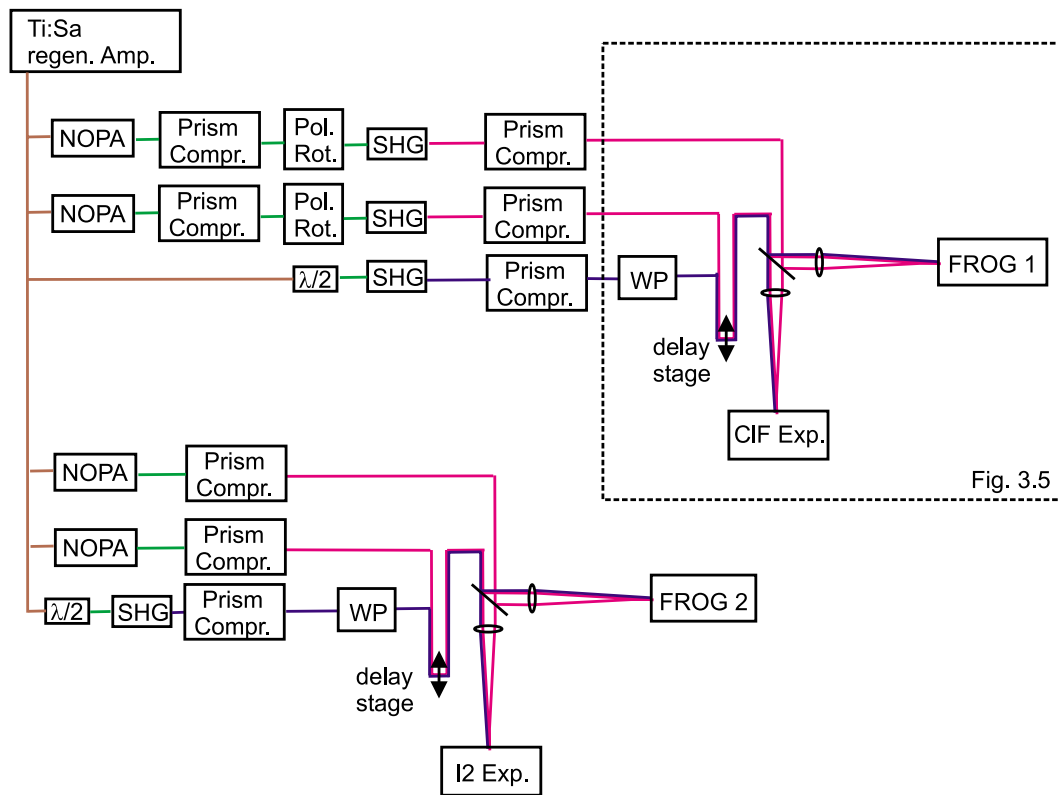


Figure 3.2: Block diagram of the laser system. The pulses are produced in the commercial regeneratively amplified Ti:Sa and split in two equal parts, one for the *CIF* experiment (upper part of the diagram) and one for the I_2 experiment (lower part). For the *CIF* experiment, there are two equal optical paths. They start with a NOPA (Fig. 3.3) to generate tunable fs pulses in the visible spectral region, pass an SF10 prism compressor and a polarization rotation stage (Pol. Rot.). The second harmonic (SHG for UV pulses) is generated and the pulses are recompressed in a quartz prism compressor, before they are directed to the sample. The polarization of the third part of the Ti:Sa output is rotated in a $\lambda/2$ waveplate. The SHG is generated and compressed in another quartz prism line. The waveplate (WP) rotates the polarization subsequently for FROG and polarization sensitive pump-probe experiments. Details of the setup in the dashed box are shown in Fig. 3.5. The setup for the I_2 experiment is similar, except that the SHG stages are missing, since the visible output of the NOPA is used.

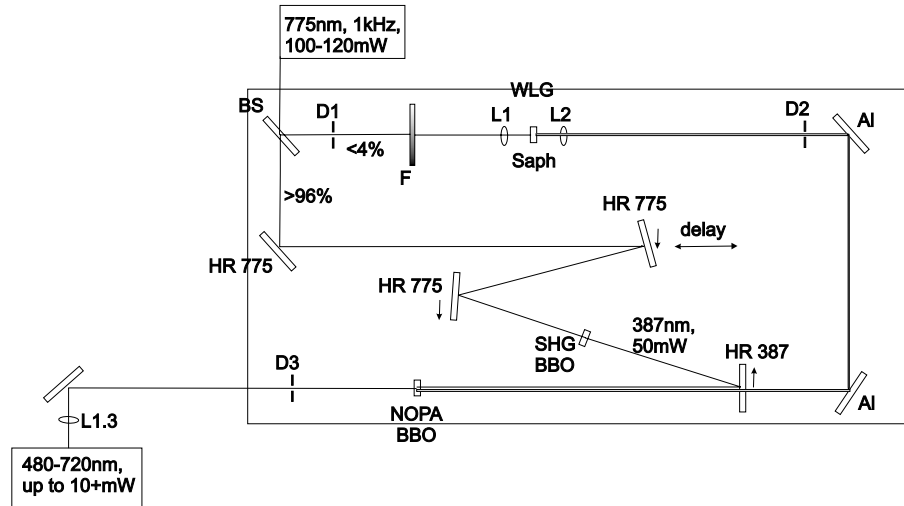


Figure 3.3: New design of the non-collinear optical parametric amplifier (NOPA). See text for an explanation.

table and aluminum mirrors are used to provide high reflectivity in the blue spectral region⁴. Three HR 775 mirrors direct the remaining 96 % of the pump light to the mirror HR 387, which is placed ~ 30 mm below the white light beam. The arrows on the mirrors indicate where the beam is lowered. The SHG BBO (1 mm thick, 5 x 5 mm cross section) is placed in the convergent beam at the position where the second harmonic efficiency (SHG) is maximal (~ 60 cm in front of the focus of the 2 m lens)⁵. The SHG efficiency is $\sim 40\%$. The plane HR 387 mirror directs the SHG beam upwards, through the NOPA BBO (2 mm thick, 5 x 5 mm), which should be placed at the position where the NOPA efficiency is optimal (~ 10 cm in front of the focus of the 387 nm beam).

The original design (commercially available from Clark) differs from the optimized setup described above. A 1 m lens in front of the NOPA reduces the beam size. The actual focusing of the 387 nm light is accomplished by a spherical focusing mirror (HR 387) with a focal length of 250 mm, which produces a hard focus just before the NOPA BBO. The SHG BBO is larger (10 x 10 mm) and the beam size on this crystal is larger, which reduces the conversion efficiency. The major improvement of the overall performance in the new design lies in the focusing conditions in the NOPA BBO, since the wave fronts of the white light and the pump light are matched better for the weak convergence induced by the lens.

3.4.2 Adjustment of the main parameters

Several parameters can be optimized to obtain pulses with specific characteristics. The wavelength tuning is accomplished by tilting the NOPA BBO and adjusting the time delay (\leftrightarrow of HR775 in Fig. 3.3) between white light and 387 nm pump light. Since the white light is positively chirped by the dispersive components, the red components come first, and the temporal overlap with the pump pulse has to be adjusted accordingly. Tilting the NOPA BBO changes the phase matching condition (Fig. 3.4) for the NOPA process (pump \rightarrow signal + idler).

The spectral width of the pulses can be influenced with the chirp of the white light and the height, at which the pump beam hits the HR 387 mirror. Additional dispersive material introduced into the white light beam induces higher positive chirp, which reduces the amplified bandwidth, because not all spectral components temporally overlap with the pump light. The position of the beam on HR 387

⁴Reflection on silver mirrors is weak below 450 nm.

⁵At this point the beam has just the size of the cheaper 5 x 5 mm BBO crystals. In the commercial NOPA setup 10 x 10 mm crystals have to be used.

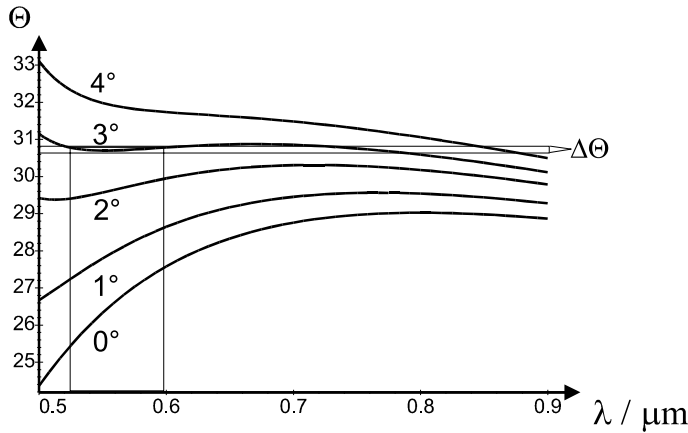


Figure 3.4: Phasematching angle Θ for different non-collinear angle $\alpha = 0, 1, 2, 3$ and 4° versus output wavelength in a NOPA pumped at $\lambda_{pump} = 387$ nm. The angle α is measured inside the BBO.

changes the non-collinear angle α . Fig. 3.4 shows the phase matching angle Θ as a function of the output wavelength λ for different non-collinear angles α [144, 185]. The 2 mm thick BBO supports a certain range of angles $\Delta\Theta$ which have a phase mismatch of less than Δk , where Δk is the argument in the sinc function [186]. Shifting the range $\Delta\Theta$ around Θ up and down in Fig. 3.4 is equivalent to tilting the NOPA BBO. In order to support a large bandwidth $\Delta\lambda$ with the phasematching condition, the proper angle α must be chosen, for which the function $\Theta(\lambda)$ is flat enough to be inside the variance $\Delta\Theta$. For the example depicted in Fig. 3.4, a range $\Delta\lambda = 500 - 600$ nm will be amplified. If the phase matching angle Θ does not vary over a wide range of wavelengths λ , not only the phase velocity ω_0/k_0 , but also the group velocity $d\omega/dk$ is matched⁶ [183]. This implies that the signal and idler pulses co-propagate through the BBO at the same speed. Therefore, the temporal broadening is minimal yielding short pulses and the efficiency of the process is increased. The non-collinear angle α not only accomplishes this group-velocity matching but also, by coincidence, the spatial walkoff of the pump and signal beam is minimized, again for the sake of efficiency in this geometry. Note that there are two symmetric geometries that realize an angle Θ of the optical axis with the pump beam. In the right configuration the angle of the optical crystal axis to the white light is larger than Θ [35].

A very sensitive parameter, as far as efficiency is concerned, is the white light generation. The beam must be optimized in order to produce a spherical and homogeneous beam profile. The intensity is adjusted with the tunable neutral density filter F in Fig. 3.3 in such a way that the white light is well (but not far) above the threshold for optimal focusing. Sometimes it is easier to use the diaphragm D1 to cut a homogeneous and spherical beam out of the 4% fundamental. For a good alignment of the NOPA, the entire intensity in the ring of parametric fluorescence generated in the NOPA BBO has to collapse into the white light beam to produce a single intense laser beam.

3.5 Generation of tunable UV femtosecond pulses

3.5.1 Pump pulses at 387 nm

The second harmonic (SHG) at 387 nm (fundamental 775 nm) is widely used throughout this work. It is produced in a 1 mm thick BBO crystal by focusing 15 % of the Ti:Sa output with a 300 mm lens and positioning the BBO approx. 5 cm before the focus. These pulses attain the theoretical limit of pulse duration dictated by the pump pulse: $\tau = 150/\sqrt{2}$ fs \approx 110 fs after compression, which is measured in a FROG autocorrelation (Fig. 3.5). The pulses are compressed in a quartz prism compressor. The efficiency of the SHG is approx. 30 %, yielding pulse energies of 34 μ J.

⁶Recall the dispersion relation $k^2(\omega) = \omega^2 n^2(\omega)/c^2$.

3.5.2 Pump and probe pulses from 240 - 360 nm

The NOPA output is frequency-doubled in a 100 μm thick BBO crystal to the range from 240 to 360 nm with pulse energies of about 1 μJ . The BBO is placed very close to the focal spot of a 300 mm lens. The bandwidth of the resulting UV pulses is limited to approx. 2 nm by the bandwidth of the SHG in the BBO crystal with thickness 100 μm . The intensity of the SHG is $I_{SHG} \sim L^2 \sin^2(\Delta k L/2)$ [98, 186]. To compress the NOPA pulses, SF10 prisms were preferred, since quartz compressors would increase the beam length by 1.5 m. For compression of the UV pulses, however, quartz prisms must be used. The spectral profile is close to Gaussian and from the Fourier transformation of the 2 nm bandwidth at 270 nm, a pulse duration of 60 fs is expected. This has been verified by a PG-FROG in CaF_2 with the 387 nm pulse as the gate (cf. chapter 3.7). UV pulses as short as 30 fs have recently been achieved in the Riedle group [187], using thinner BBO crystals. This has not been implemented during this work, since the conversion efficiency is reduced. In addition, the increased spectral bandwidth limits the time resolution in the pump probe spectra, if the potentials are strongly anharmonic. The large variation in the shape of the pump-probe spectra in Fig. 6.8 upon tuning the probe wavelength by only 2 nm indicates that spectrally broader pulses would smear out the spectra. Moreover, the time resolution in the B state spectra is limited by the pulse duration of the 387 nm pulse. In the future, however, it will be worthwhile to generate shorter pulses for experiments with $^1\Pi$ excitation, i.e. when the second harmonic of the NOPA can be used for pump and probe pulses⁷.

3.6 Pump-probe and FROG setup

Fig. 3.5 shows the multi-purpose optical setup, which is used to characterize all femtosecond pulses and to perform the pump-probe experiments. In addition, the time zero, i.e. the time coincidence $\Delta t = 0$ of pump and probe on the sample, can be measured with this setup. First the upper half of the setup is described. The three boxes labeled SHG of NOPA1, SHG of NOPA2 and SHG of Ti:Sa indicate the three independent UV pulses described above, each after running through the UV prism-compressors mentioned in Fig. 3.2. In the following they are referred to as λ_{N1} , λ_{N2} and λ_{Ti} . Note that all pulses are polarized parallel (\leftrightarrow) to the optical table, since this allows the prism compressors to run in Brewster angle configuration, which minimizes the reflection losses and in addition improves the degree of linear polarization. If the beams are properly aligned, i.e. are parallel to the optical table, no additional polarizer is needed to improve the polarization⁸. On the dichroic mirror DM, which is a high reflector for 387 nm on a quartz substrate, the beams λ_{N1} and λ_{Ti} are overlapped and they co-propagate subsequently. The beamsplitter BS is mounted in a flip-holder and is inserted for pulse characterization with autocorrelation FROG. The retroreflector (R) is mounted on a delay stage that can be moved with a computer-controlled stepping motor with 1 step corresponding to 1 μm , i.e. 0.66 fs (the beam travels additional 2 μm when the mirror is displaced by 1 μm). The beam λ_{N2} tightly passes mirror M1, and the beams are aligned in such a way that λ_{N2} propagates parallel to the two other beams at a distance of approx. 8 mm. If the waveplate WP is inserted into the setup, it rotates the polarization of λ_{N1} or λ_{Ti} . The flip-mirror FM determines, whether the pulses continue to the external FROG setup in the dotted frame or to the sample chamber where the FROG can be measured "in situ" and where the pump-probe experiments are executed. The identical quartz lenses L_1 and L_2 have a focal length of 100 mm and a copy of the entrance window of the sample chamber provides the same dispersion in the external FROG setup.

⁷Then quartz prisms will have to be used to compress the NOPA light. Otherwise higher order chirp will limit the pulse duration.

⁸If the beam is reflected up and down, i.e. not symmetrical with respect to the polarization vector, metal mirrors induce elliptical polarization.

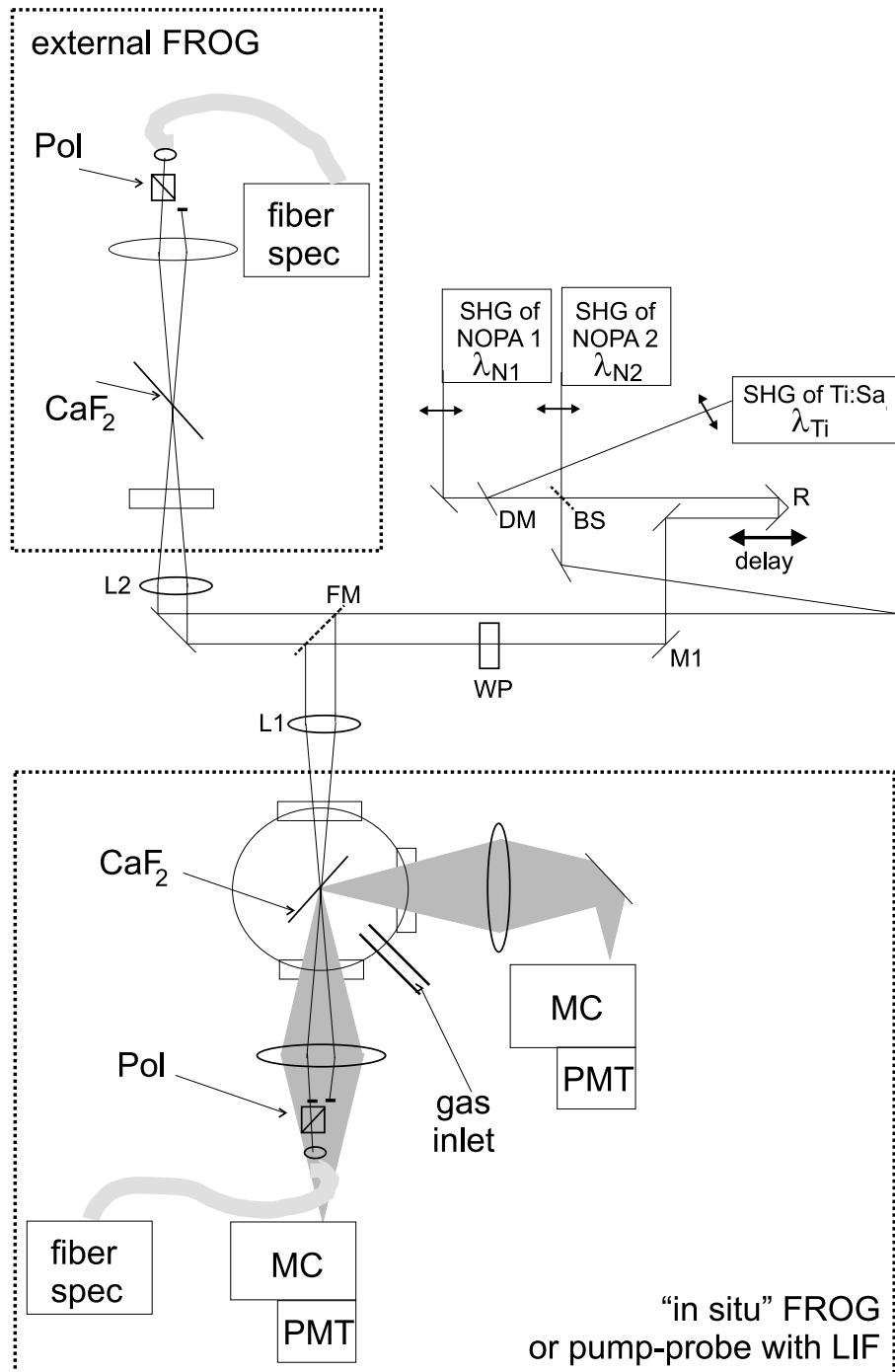


Figure 3.5: Combined pump-probe and FROG setup. Frame external FROG: A signal and a gate beam are focused on the CaF_2 substrate. The signal beam passes the polarization analyzer (Pol) and is spectrally resolved in the fiber optic spectrometer (fiber spec.). Without frame: Three horizontally polarized beams, λ_{N1} , λ_{N2} and λ_{Ti} are provided (see Fig. 3.2). The beam splitter BS and the mirror FM are mounted on flip-holders. BS is only introduced for FROG autocorrelations. FM is flipped out of the laser beams to run the external FROG. Frame "in situ" FROG: identical setup as for external FROG. Here the CaF_2 substrate is in the center of the sample chamber, and the fluorescence can be detected in the forward direction and at 90° with a monochromator (MC) and a photomultiplier tube (PMT). The polarizer (Pol) and the fiber spectrometer for the FROG have to be removed, when fluorescence in the forward direction is recorded. The gas inlet shows the thin tube for the doped rare gas used to grow the samples on the CaF_2 substrate.

3.7 Pulse characterization and determination of time zero

The pulses are characterized by the Polarization-Gating Frequency Resolved Optical Gating technique [188, 189] (PG-FROG). The setup implemented in this thesis allows the characterization of fs pulses from IR to UV (Fig. 3.5). It owes its flexibility to the use of a fiber optic spectrometer as a wavelength resolving detector. The visible pulses from the NOPAs, the Ti:Sa fundamental and its second harmonic are measured by autocorrelation, i.e. the pulses are split into two copies at the beamsplitter BS, one pulse serving as the "signal" beam and one as the "gate" [190]. The pulses are delayed with the same stage as in the pump-probe experiments and focused onto the 1 mm thick CaF_2 substrate (nonlinear FROG medium) in the sample chamber or alternatively on an equivalent CaF_2 outside⁹. The frequency doubled NOPA pulses are too weak to characterize them by autocorrelation. For them cross-correlation with a well characterized and strong 387 nm pulse is used by flipping the beamsplitter BS down. The duration of the 387 nm pulse limits the time resolution of the FROG cross correlation¹⁰. In all FROG measurements the "signal" pulse is linearly polarized, passes a polarization analyzer POL after the FROG medium and is focused into the fiber optic spectrometer (cf. chapter 3.8). The $\lambda/2$ waveplate (WP) turns the linear polarization of the gate pulse to approx. 45° with respect to the signal pulse. If the pulses overlap in space and time inside the FROG medium, the nonlinear susceptibility $\chi^{(3)}$ induces polarization components in the signal beam that pass the polarization analyzer (POL). The intensity of these components, $I_{FROG} \sim I_{signal} I_{gate}^2$ is proportional to the intensity of the "signal" pulse I_{signal} and to the square of the intensity of the gate I_{gate} . By scanning the delay between signal and gate, a two dimensional FROG trace is generated that shows the intensity of the pulse as a function of frequency and time. The chirp (frequency modulation) of the pulse can be read directly from the FROG trace [32, 144, 190]. In this thesis only transform limited pulses are used; however, this setup allows the characterization of shaped pulses in future experiments.

The time zero of the pump-probe experiment is given as the center of the cross correlation, i.e. the projection of the FROG trace onto the time axis. When the cross correlation FROG is measured in the sample chamber, a pump-probe spectrum can be taken in the same scan, when the LIF is collected at 90° (see below). This allows a very precise measurement of the time zero in the pump-probe spectra with an uncertainty of $\Delta t = \pm 20$ fs. In the experiments involving two frequency doubled NOPA pulses, the time zero must be inferred from the pump-probe spectrum itself. This is usually not difficult, since for equal pump and probe wavelength the spectrum is symmetric and for different wavelengths a minimum is clearly visible.

3.8 Fluorescence detection

The lower portion of Fig. 3.5 shows the sample chamber with the setup for fluorescence detection. The laser beams are focused onto the rare gas sample on top of the CaF_2 substrate, which can be rotated and is usually kept tilted at 45° . In this configuration, the fluorescence can be detected simultaneously in the forward direction and perpendicular to the incoming beams to reduce stray light.¹¹

In one set of experiments, the fluorescence is excited with a $XeCl$ excimer laser at 308 nm (typical parameters: pulse duration $\Delta t = 10$ ns, repetition rate 10 Hz, pulse energy $W = 200 \mu J$, focus

⁹To find the signal it is helpful to first find the spacial overlap with a pinhole. In some cases a 1 mm sapphire window is used, but the FROG signal often saturates even on the thin 300 μm sapphire window.

¹⁰If UV pulses as short as 30 fs are to be characterized, one will have to resort to other techniques like downconversion in very thin BBO crystals. The 775 nm pulse cannot be used because of the large group velocity difference to the UV pulses.

¹¹It turns out in the experiments that all fluorescence bands of ClF/Ar are isotropic and unpolarized. This reflects the fact that the molecules undergo strongly hindered rotation within the fluorescence lifetime or that they are randomly tilted after scattering events. A different situation is met in the case of I_2/Kr and Cl_2/Ar , which are sterically fixed. Here the fluorescence is emitted with polarization parallel to the exciting polarization ($\Delta\Omega = 0$), implying emission with a dipole characteristic.

diameter $d = 2$ mm). The corresponding mirrors and the lens are not shown in Fig. 3.5, but beam propagates in the direction of the shown laser beams. This yields the valence band emission $A' \rightarrow X$. The ion-pair emission $D' \rightarrow A'$ is accessed by excitation with two photons, e.g. by using higher repetition rate or tighter focusing. The tunable fs laser pulses from two frequency doubled NOPAs (λ_{N1} and λ_{N2}) are used alternatively to produce the A' and D' emission or the excimer emission of Kr_2F . The second harmonic at 387 nm of the Ti:Sa regenerative amplifier system accesses only the valence states of ClF , also generating the A' emission.

For frequency domain spectroscopy, the fluorescence from the sample is collimated with a 100 mm fused silica lens onto a fiber optic spectrometer (fiber spec)¹². It has a resolution of 0.7 nm for the large wavelength range from $\lambda = 350$ to 1050 nm and of 0.3 nm for the range extending from 200 to 530 nm. The integration time is 50 ms. For decay time measurements, the time window is delayed with respect to excitation. Contributions on shorter time scales are checked using either a CCD camera with a time resolution of 1 μ s, or a photomultiplier tube (PMT) behind a monochromator (MC). Two monochromators (MC) with PMTs are used in pump-probe experiments to record different fluorescence bands simultaneously. One of the monochromators can be scanned with an electronic control unit. The UV fluorescence spectra were taken with this setup. For very strong emissions the fiber optic spectrometer can also be used.

For I_2 in Kr , the sample is perpendicular to the incoming beams and the fluorescence is detected in the forward direction using a combination of color glass filters and a monochromator before the photomultiplier. The fluorescence around 420 nm consists of two contributions [80] belonging to the $D' \rightarrow A'$ and the $\beta \rightarrow A$ or $\delta \rightarrow A$ transitions and both bands were detected together. The details can be found in the two respective diploma theses [116, 144].

3.9 Pump-probe setup

For time domain spectra, the fluorescence is collimated onto two monochromators with photomultiplier tubes, one in forward direction and one perpendicular to the laser beams, in order to monitor two bands at the same time. The photo current is amplified by the factor 100 and 1000, respectively, before it is integrated in a box car. The analog box car output is digitized with a DAC card and fed into the computer. One data point in a pump-probe spectrum is typically an average over 1000-8000 laser pulses, depending on the noise level and the time constraints due to bleaching of the sample. The setup is also used to measure time domain spectra with the full wavelength information of the fiber spectrometer when the intensity of the fluorescence is strong enough. Then the setup resembles the setup for FROG measurements but without the polarization analyzer POL (chapter 3.7). The fluorescence, instead of the "signal" pulse, is focused into the fiber optic spectrometer.

Pump and probe pulse are delayed with respect to each other on a delay stage which can be moved by a computer controlled stepping motor (Fig. 3.5). For the ClF and Cl_2 spectra, the pump pulse was either the second harmonic of the Ti:Sa at 387 nm or a frequency doubled NOPA (240 - 330 nm). The second frequency doubled NOPA served as the probe pulse. For I_2 experiments two NOPA pulses were used after pulse compression in a quartz prism sequence.

In the pump-probe spectra that involve probing KrF , there is a large delay-independent background, since vibrationally relaxed KrF is also probed. Therefore a software "lock-in" technique was implemented; a synchronized light beam chopper (model 221 from HMS Elektronik) blocks every second pump pulse. The computer then subtracts the signals with probe pulses only from the ones with pump and probe pulse. This method greatly improves the signal to noise ratio. Some comments on the "lock-in" signal and its interpretation are given in the Appendix. This technique will be useful

¹²The SD2000 fiber optic spectrometer from Ocean Optics is also used for the FROG measurements. For the spectroscopy the polarization analyzer POL is removed.

in future experiments, whenever an unwanted, delay-independent signal from metastable states (e.g. A' state of ClF) exists.